# Lecture 19

# Planetary magnetospheres

The **Aim** of this Lecture is to compare the magnetospheres of planets in our solar system, describing the similarities and differences, and to explore the solar wind's interactions with unmagnetized planets.

The first part of this lecture compares the magnetospheres of the six magnetized planets in the solar system. Features such as magnetospheric size, plasma sources, and dynamics are considered. The second part considers the interaction of the solar wind with unmagnetized bodies. Two examples are addressed: (1) Earth's moon, which is a poor conductor, and is thus unable to magnetically deflect the solar wind, and (2) Venus, which possesses an electrically conducting ionosphere which enables it to deflect the solar wind flow. The region around which the solar wind is deflected has many similarities to a planetary magnetosphere.

**Expected Learning Outcomes.** You are expected to be able to

- Explain how the corotation electric field and imposed solar wind convection electric field vary with distance from a magnetized planet.
- Explain how the size of planetary magnetospheres depends on the magnetopause current layer, the planet's dipole field, the strength of the magnetodisk and/or plasmasheet current layer, and the solar wind ram pressure.
- Explain qualitatively why magnetospheric plasma sources can substantially affect the characteristics of a magnetosphere.
- Compare the sizes and magnetospheric dynamics of the magnetized planets in terms of the above concepts.
- Explain qualitatively how an unmagnetized planet or moon can develop a global or localized bow shock.
- Describe the role of the Venusian ionopause, explaining the physics of its current layer and how it plays the same role as a magnetopause.
- Describe how magnetic field lines can become draped over a conducting obstacle (like an ionopause or magnetopause), increasing the magnetic field there.

## 19.1 Comparison of planetary magnetospheres

### Magnetospheric size

It was demonstrated in Lecture 13 that the distance $r_{mp}$ of the magnetopause from Earth along the Earth-Sun line can be estimated quite accurately using static

pressure balance arguments, where the total pressure of the magnetosheath and magnetospheric plasmas balance across the magnetopause. We briefly review these arguments here.

The supersonic solar wind ram pressure usually well exceeds the thermal and magnetic pressures, so that the total pressure of the solar wind plasma incident on the bowshock satisfies

$$p_{sw} = \eta_{sw} U_{sw}^2 \,. \tag{19.1}$$

The supersonic solar wind becomes subsonic in the magnetosheath, and the flow speed is nearly zero at the magnetopause. Hence, from the equation for conservation of normal momentum (sometimes described as total pressure) [see equations (2.25) and (13.2)], the ram pressure is almost totally converted into thermal and magnetic pressure. Assuming that this conversion is 100% efficient, the total pressure in the magnetosheath plasma just in front of the magnetopause satisfies

$$p_{sh} = p_{th,sh} + p_{B,sh} = \eta_{sw} U_{sw}^2 \,. \tag{19.2}$$

On the other side of the magnetopause, in the magnetosphere, the dominant term in the pressure balance equation is the magnetic pressure. The magnetic field strength $B_{ms}$ just inside the magnetopause boundary is the sum of the planetary dipole field and the field induced by the current layer in the magnetopause (see Lecture 13) with

$$B_{ms}(r_{mp}) = 2B_{eq} \left( \frac{R_P}{r_{mp}} \right)^3 \,, \tag{19.3}$$

where $R_P$ is the radius of the planet, $B_{eq}$ is the equatorial surface magnetic field, and $r_{mp}$ is the distance to the magnetopause. In steady state pressure balance $p_{sh} = p_{ms}$ is satisfied across the magnetopause boundary. Substituting in equations (19.2) and (19.3),

$$\eta_{sw} U_{sw}^2 = \frac{B_{ms}^2}{2\mu_0} \,. \tag{19.4}$$

Thus, the distance to the magnetopause is

$$\frac{r_{mp}}{R_P} = \left( \frac{2B_{eq}^2}{\mu_0 \eta_{sw} U_{sw}^2} \right)^{1/6} \,. \tag{19.5}$$

The solar wind flow speed $U_{sw}$ is approximately constant with distance from the Sun if the effects of fast and slow streams, CMEs, and pickup ions are ignored (see Lectures 11 and 20). Then the predicted magnetospheric size depends on the plasma density $\eta_{sw}$, which varies as the inverse square of the distance from the Sun, and the strength of the effective planetary magnetic field.

Table 19.1 compares the predicted and observed values of $r_{mp}$. It is evident from Table 19.1 that the estimated magnetospheric sizes derived from pressure balance arguments are consistent with the observed values, except for Jupiter.

Simple pressure balance arguments are not adequate to treat Jupiter's magnetosphere, because of the Io torus, dense plasma sheet and resulting "magnetodisk" (Lecture 18). In Earth's magnetotail initially dipolar magnetic field lines are stretched tailwards by the effects of the solar wind and ionospheric outflow, leading to a current sheet around the neutral line (with direction given by Ampere's Law). The direction of this current turns out to be consistent with the directions of the $\nabla B$ and curvature drifts, which give rise to the ring current. You may remember that the ring current generates a magnetic field that opposes the Earth's field interior to the ring but adds at the magnetopause where it is exterior to the ring.

Something very similar occurs at Jupiter. Now, however, the corotation electric field dominates and magnetic field lines in the (corotating) Io plasma torus are

| | Mercury | Earth | Jupiter | Saturn | Uranus | Neptune |
|---|---|---|---|---|---|---|
| Distance $(10^{10}\,\mathrm{m})$ | $4.7-7.0$ | 15 | 78 | 140 | 290 | 450 |
| $\eta_{sw}\,(10^{-23}\,\mathrm{kg\,m^{-3}})$ | $5800-13000$ | 1300 | 50 | 17 | 3.3 | 1.3 |
| $R_P\,(10^6\,\mathrm{m})$ | 2.4 | 6.4 | 71 | 60 | 26 | 25 |
| $B_{eq}\,(10^{-5}\,\mathrm{T})$ | 0.003 | 3.1 | 43 | 2.2 | 2.3 | 1.4 |
| $\frac{r_{mp}}{R_P}$ (predicted) | $1.4-1.6$ | 9.5 | 39 | 17 | 23 | 23 |
| $\frac{r_{mp}}{R_P}$ (observed) | 1.4 | $8-12$ | $50-100$ | $16-22$ | 18 | $23-26$ |

Table 19.1: Comparison of observed and predicted magnetopause distances for the magnetized planets (adapted from Kivelson and Bagenal, 1999).

stretched outwards at **all longitudes** by centrifugal forces due to Jupiter's rapid rotation. Physically the associated currents must lead to a field that opposes the imposed planetary field, since plasmas are diamagnetic. Consider the MHD equation of motion (2.25) in the frame of reference corotating with Jupiter's magnetosphere at constant angular velocity $\mathbf{\Omega}$,

$$\eta\left[\frac{\partial \mathbf{U}}{\partial t}+(\mathbf{U}\cdot\boldsymbol{\nabla})\mathbf{U}+\mathbf{\Omega}\times(\mathbf{\Omega}\times\mathbf{r})+2(\mathbf{\Omega}\times\mathbf{U})\right]=-\nabla p+\mathbf{J}\times\mathbf{B}\,. \tag{19.6}$$

The two additional terms on the left-hand side correspond to the centrifugal and Coriolis forces respectively in this non-inertial frame of reference. Assuming a steady flow, and that the Coriolis force is small relative to the centrifugal force, equation (19.6) reduces to

$$\mathbf{J}\times\mathbf{B}=\nabla p+\eta\mathbf{\Omega}\times(\mathbf{\Omega}\times\mathbf{r})\,. \tag{19.7}$$

Taking the radial component (with the directions of $\mathbf{J}$ and $\mathbf{B}$ as shown in Figure 19.1), one finds that

$$J_\phi B=-\frac{\partial p}{\partial r}+\eta\Omega^2 r\,. \tag{19.8}$$

The pressure gradient and centrifugal forces in the plasma sheet in the radial direction are balanced by an inward-directed $\mathbf{J}\times\mathbf{B}$ force, as shown in Figure 19.1. The azimuthal current $J_\phi$ is the magnetodisk current (similar to the heliospheric current sheet and the tail current at Earth). Note that the $\nabla B$ and curvature drifts lead to currents in the same direction (consistent with Lenz's law). It is easy to show that the magnetodisk current enhances the dipole magnetic field at distances beyond the magnetodisk but opposes the dipole field at smaller distances.

The enhanced size of Jupiter's magnetosphere relative to the predictions in Table 19.1 is thus caused by the enforcement of corotation to large distances and the enhanced plasma pressure due to the plasma sheet and Io plasma torus, both of which lead to an current in the magnetodisk and an enhanced magnetic pressure at the magnetopause. The observed scaling of the magnetopause location with solar wind ram pressure is consistent with this conclusion, as shown by E. Smith, J.A. Slavin and co-workers.

The huge extent of Jupiter's magnetosphere can be appreciated by considering that if the magnetosphere of Jupiter could be seen in the sky at Earth, its maximum angular size would be twice that of the Sun, even though Jupiter is at least four times further away from Earth than from the Sun. Moreover, Jupiter's magnetotail is over 6 AU long and extends beyond the orbit of Saturn.

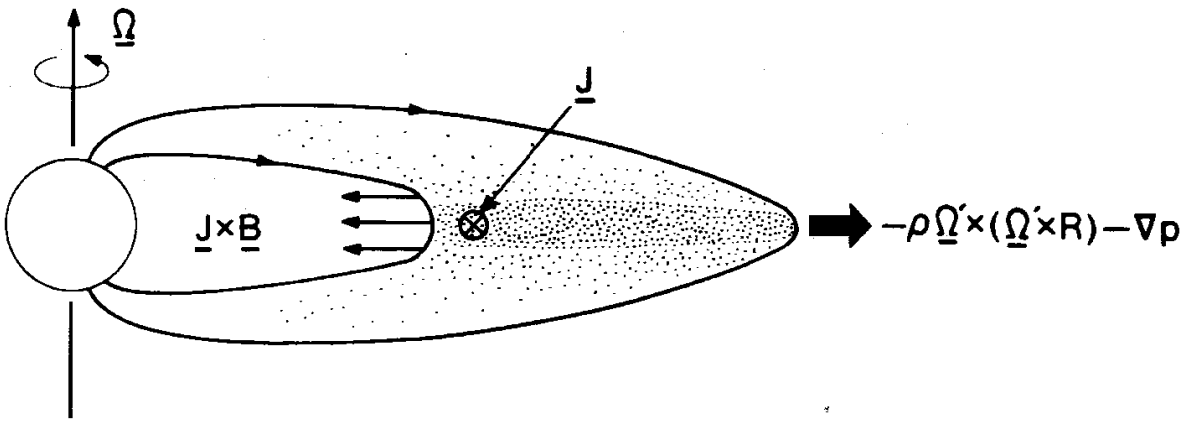


Figure 19.1: Radial force balance in the jovian plasma sheet (Cravens, 1997).

## Magnetospheric dynamics

Large-scale motions in planetary magnetospheres are dominated by $\mathbf{E} \times \mathbf{B}$ drifts associated with convection and corotation electric fields. In Earth's magnetosphere, $\mathbf{E}$ is the convection electric field associated with the solar wind flow. The direction of $\mathbf{E}$ is given by $-\mathbf{U} \times \mathbf{B}$. and the magnitude can be written

$$E_{cv,sw} = \alpha U_{sw} B_{IMF} \ . \tag{19.9}$$

Here $\alpha$ is the efficiency of dayside magnetic reconnection, which depends on the orientation of the IMF, and $B_{IMF}$ is the interplanetary magnetic field strength.

The *corotational electric field* was discussed in detail in Lecture 18. The region of corotating plasma is called the plasmasphere (see Lecture 14). In the rest frame of the Sun-planet line, the corotating magnetospheric plasma sets up a corotational electric field $\mathbf{E}_{cor}$, which corresponds to equation (19.9) with flow velocity $\mathbf{U} = \mathbf{\Omega}_P \times \mathbf{r}$, where $\mathbf{\Omega}_P$ is the angular frequency of the planet and $\mathbf{r}$ is the radial position vector:

$$\mathbf{E}_{cor} = -(\mathbf{\Omega_P} \times \mathbf{r}) \times \mathbf{B} \, . \tag{19.10}$$

Assuming a dipole planetary magnetic field whose magnetic axis is perpendicular to the equatorial plane, and assuming that $\mathbf{r}$ lies in the equatorial plane, $\mathbf{E}_{cor}$ for planet $P$ is directed radially inwards or outwards (depending on the dipole sense) with magnitude

$$E_{cor} = \frac{\Omega_P B_{eq} R_P^3}{r^2} \, . \tag{19.11}$$

Comparison of the relative magnitudes of the solar-wind-driven convection electric field (19.9), which is relatively constant throughout the magnetosphere, and the corotational electric field (19.11), which decreases as the square of the distance from the planet, determines where the magnetosphere's dynamics are dominated by the solar wind or the planet's rotation. The plasmapause distance $r_{pp}$ corresponds

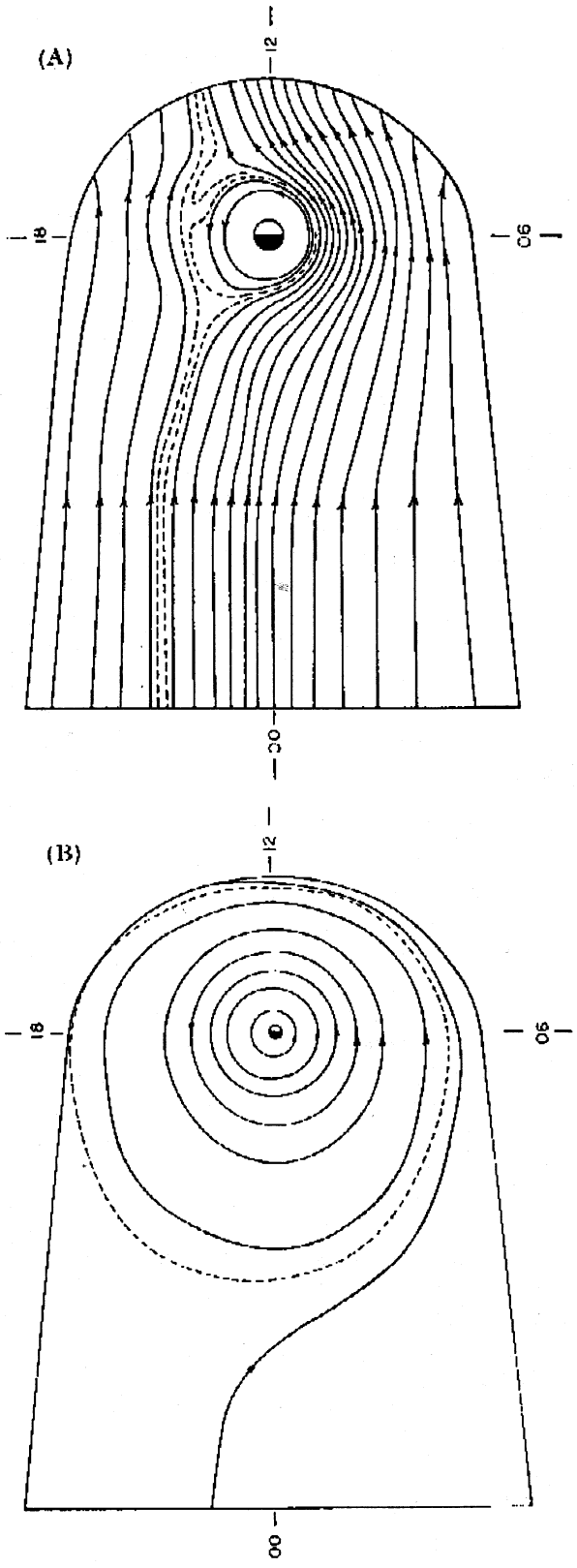


Figure 19.2: Plasma flow directions in the ecliptic plane of (A) Earth's magnetosphere, and (B) Jupiter's magnetosphere (Brice and Ioannidis, 1970). The position of the plasmapause is denoted by the dashed line.

to where the condition $E_{cor} = E_{cv}$ is satisfied. The corotational electric field dominates for $r < r_{pp}$ where the plasma corotates with the planet, and the convection electric field dominates for $r > r_{pp}$. An expression for $r_{pp}$ is obtained by equating (19.9) and (19.11), with

$$\frac{r_{pp}}{R_P} = \sqrt{\frac{\Omega_P B_{eq} R_P}{\alpha U_{sw} B_{IMF}}} \,. \tag{19.12}$$

If $r_{pp} < R_p$, where $R_P$ is the planet's radius, then the convection electric field dominates everywhere and corotation is unimportant. Substituting in typical solar wind parameters at Earth, one finds $r_{pp}/R_E = 5.5$, and this value corresponds to the observed position of the plasmapause in the equatorial plane. The distance to Earth's magnetopause is $r_{mp}/R_E \approx 10$. Thus the plasmasphere comprises only a small fraction of the total volume of Earth's magnetosphere. As a result, the dynamics in most of Earth's magnetosphere is dominated by the solar wind (see Lecture 15).

For Jupiter, one finds $r_{pp}/R_J = 240$ which, in fact, exceeds the maximum observed distance to the magnetopause ($100R_J$). Thus, in Jupiter's equatorial plane corotation is the dominant effect all the way out to the magnetopause. Solar wind convection electric fields do, in fact, play a role at higher latitudes and in the magnetotail, but, on the whole, corotational electric fields dominate. Typical flow patterns of plasma in the ecliptic plane for Earth's and Jupiter's magnetospheres are shown in Figure 19.2. Similar results are found for the other giant planets as for Jupiter - the dynamics are dominated by corotation electric fields.

Another important factor in magnetospheric dynamics is the orientation of the magnetic and spin axes relative to the ecliptic plane. These angles are shown for Earth and the giant planets in Figure 19.3. When the magnetic and rotation axes are both nearly perpendicular to the ecliptic plane, which is the case for Earth, Jupiter and Saturn, then the $\mathbf{E} \times \mathbf{B}$ flows are quasi-steady for constant solar wind conditions. Larger angles between the spin and magnetic axes correspond to more variation in the dynamics over one planetary rotation. This effect is most dramatic for Uranus and Neptune, where the orientation of their magnetic fields varies with respect to the solar wind flow and IMF over each rotation period. As a result the dynamics of Uranus and Neptune's magnetospheres are complex.

For Uranus, the rotation axis is presently nearly aligned with the solar wind direction. As for Jupiter, most of the magnetospheric plasma corotates with Uranus. In the reference frame corotating with Uranus, in which the corotational electric field is zero, solar-wind-driven convection similar to that in Earth's magnetosphere occurs over time scales of days. There is also a longer seasonal variation, corresponding to where the orientation of the rotation axis relative to the IMF and solar wind flow varies over Uranus's 84-year orbit of the Sun.

Figure 19.4 shows the magnetosphere of Neptune, where neither the spin nor the rotation axes are aligned perpendicular to the ecliptic plane or with the solar wind direction. There is no reference frame in which the flow is quasi-steady. The two configurations shown in Figure 19.4 are half a rotation period apart. One example of the time-varying dynamics is that the reconnection rate at the magnetopause is significantly lower in the second configuration, where a smaller area of the magnetopause has field lines antiparallel to the IMF direction.

## Magnetospheric plasma sources

Recall from Lecture 14 that there are two sources of plasma in Earth's magnetosphere: (1) the solar wind, where solar wind material enters the magnetosphere via the magnetosheath through the cusp regions and during magnetic reconnection

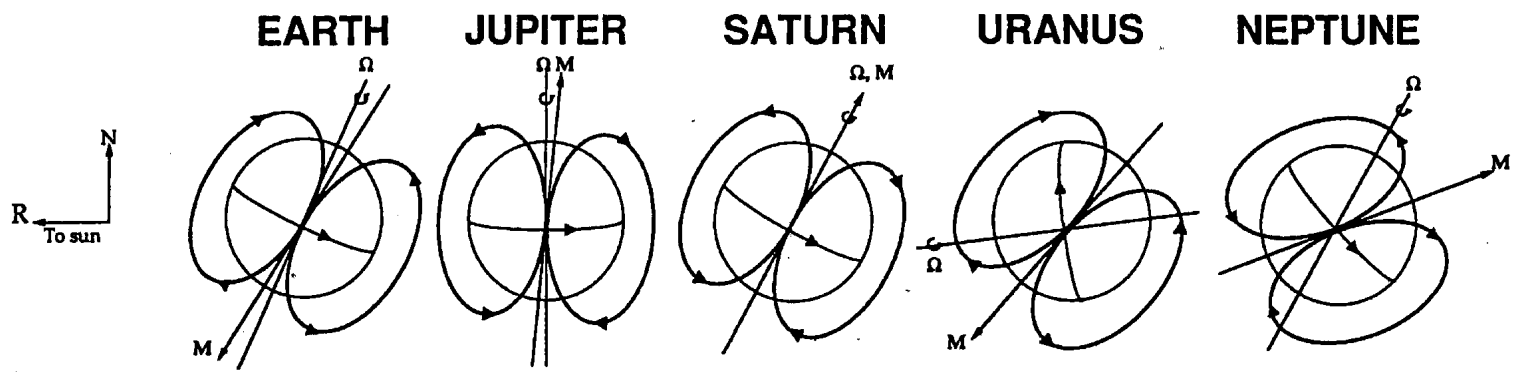


| | EARTH | JUPITER | SATURN | URANUS | NEPTUNE |
|---|---|---|---|---|---|
| Obliquity $\cos^{-1}(\Omega \cdot N)$ = | 23.5° | 3.1° | 26.7° | 97.9° | 29.6° |
| Dipole Tilt $\cos^{-1}(\Omega \cdot M)$ = | +11.7° | -9.6° | -0.0° | -59° | -47° |
| Solar Wind Angle $\cos^{-1}(\Omega \cdot R)$ = | 66.5 - 113.5° | 86.9 - 93.1° | 63.7 - 116.5° | 7.9 - 172.1° | 60.4 - 119.6° |

Figure 19.3: Orientation of spin and magnetic axes relative to the ecliptic plane for Earth, Jupiter, Saturn, Uranus and Neptune [Baganel, 1992].

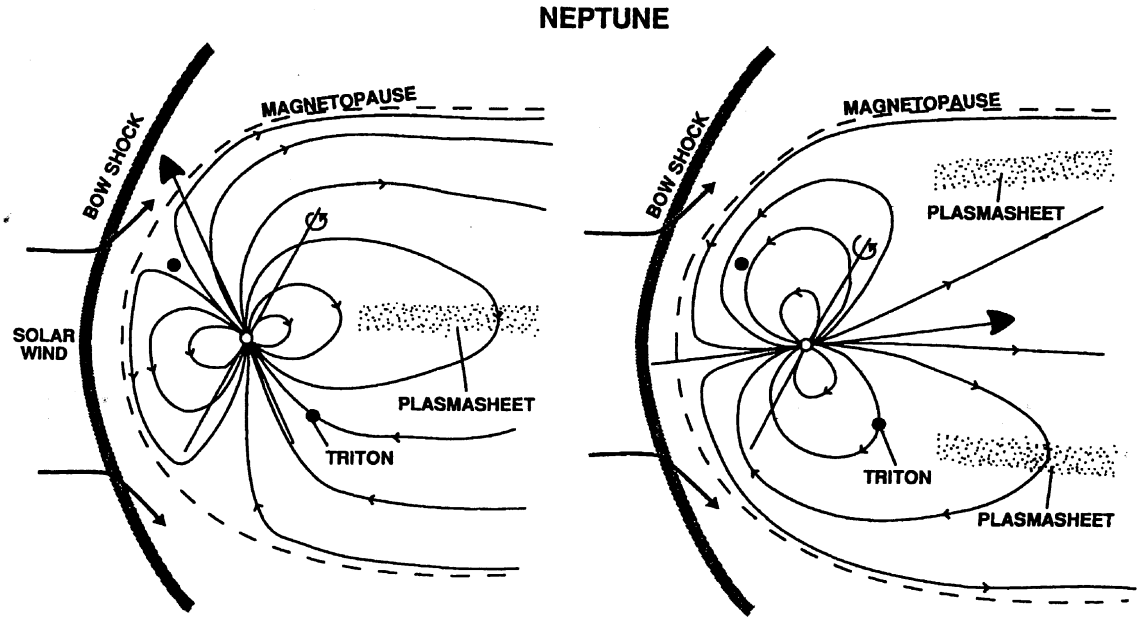


Figure 19.4: The magnetosphere of Neptune, at two times separated by half the rotation period (8 hours) [Baganel, 1992].

events; and (2) the ionosphere, where a small fraction of ionospheric plasma escapes Earth's gravity into the plasmasphere.

The predominant ion species in Jupiter's inner magnetosphere are sulphur and oxygen ions. The main plasma source for the jovian magnetosphere is the volcanically active moon Io, where atoms from Io's sulphur dioxide atmosphere escape Io's gravitational attraction by magnetospheric particle sputtering, and are subsequently impact ionized (see Lecture 18). Earth and Jupiter have the densest magnetospheres in the solar system, with maximum particle densities $> 1 \times 10^9\,\mathrm{m}^{-3}$.

The predominant ion species in Saturn's inner magnetosphere are $H^+$, $O^+$, and $H_2O^+$, which suggests that energetic particle sputtering of material from Saturn's rings and icy satellites Dione and Tethys is the main plasma source. It has also been postulated that the moon Titan contributes nitrogen ions to the outer magnetosphere. Titan's orbit (20.3 $R_S$) lies in between the minimum and maximum observed magnetopause distances at Saturn ($16 < r_{mp}/R_S < 22$) and so Titan spends part of its time outside Saturn's magnetosphere. In the inner magnetosphere there is evidence of interactions between magnetospheric plasma and ring material. The study of dusty plasmas, which is applicable to this situation, is a relatively new field in plasma physics. The density of Saturn's magnetosphere is an order of magnitude lower than for Jupiter and Earth, with maximum particle densities $\approx 1 \times 10^8\mathrm{m}^{-3}$.

Both Uranus and Neptune have relatively diffuse magnetospheres, with maximum particle densities $\approx 3 \times 10^6\mathrm{m}^{-3}$. The main source of Uranus's magnetosphere (predominantly $H^+$ ions) are ionospheric outflows and electron impact ionization of Uranus's hydrogen atmosphere. For Neptune, the moon Triton provides nitrogen ions. Low sputtering rates are predicted from the icy satellites of Neptune.

## 19.2 Solar wind flow around unmagnetized bodies

Magnetized bodies deflect the solar wind, and the flow speed varies from supersonic to subsonic across the bow shock. At Earth, the bow shock typically stands off at distances of $10R_E$, well beyond Earth's atmosphere and ionosphere. What happens in situations where the deflecting body does not possess a magnetic field? To answer this question, the category of unmagnetized bodies needs to be further divided into bodies with low or high electrical conductivities. We discuss two examples: Earth's Moon and Venus.

### The Moon

The Moon has no atmosphere or intrinsic magnetic field on a global scale and is a poor conductor. Solar wind particles thus collide directly with the lunar surface and are absorbed. Interplanetary magnetic field lines pass easily through the Moon. It is thus impossible for a pressure build-up (thermal or magnetic) to form in front of the moon and so a bow shock is not generated. A wake is produced directly behind the Moon along $\mathbf{v}_{sw}$, while absorption of impacting particles by the Moon leads to shadown regions that are "inverse" foreshocks defined by magnetic connection to the Moon and time-of-flight effects.

Localized magnetic dipoles associated with "masscons" (mass concentrations) have been observed on the Moon by the spacecraft Lunar Prospector. Recent simulations by R. Winglee and E. Harnett (U. Washington, USA) suggest that localized bow shocks with scales $\approx 0.1R_M$ form when these dipoles are exposed to the solar wind flow. These localized bow shocks have "mini-magnetospheres" and, arguably, foreshock regions with detectable plasma waves and radio emissions.

## Venus

The plasma environment around Venus, which possesses a conducting ionosphere, is shown in Figure 19.5. The boundary between Venus's ionosphere and the solar wind

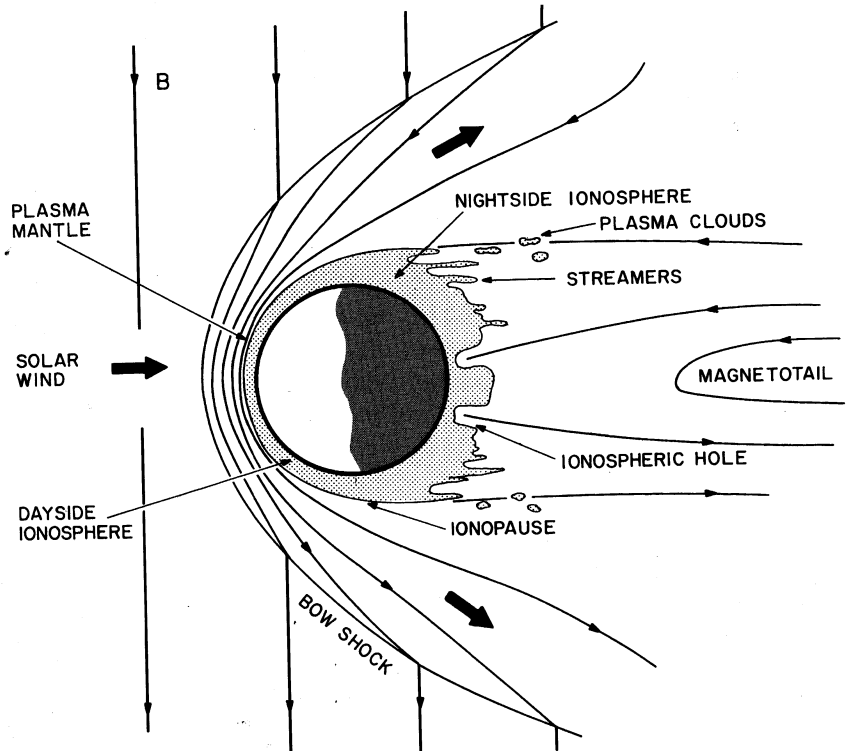


Figure 19.5: Schematic of the plasma environment of Venus (Cravens, 1997).

plasma is called the *ionopause*. The supersonic solar wind must become subsonic at some location upstream of the ionopause, and this marks the position of the bow shock.

What is the physics of the ionopause? It turns out to be essentially identical to the magnetopause and its current layer discussed in Lecture 13. Very simply, the ionosphere is essentially unmagnetized but hot, while the solar wind is magnetized: accordingly, in the frame of the solar wind plasma, the unmagnetized ionospheric plasma flows towards the magnetized region and produces a current layer as described in Lecture 13. That is, the ionospheric ions and electrons try to stream across the ionopause but now feel the magnetic field and execute half a gyroorbit before returning to the ionosphere travelling in the oposite direction. The associated currents lead to a $\mathbf{J} \times \mathbf{B}$ force that numerically equal the gradient of the ionosphere's thermal pressure, causing the thermal ionospheric plasma to remain interior to the ionopause. Currents associated with solar wind plasma moving into the ionosphere leads to essentially the same effect, causing the two plasmas to remain separate (as required by the frozen-in magnetic field conditions, at least where the ionosphere is sufficiently conducting and collisionless).

Thus, in general an ionopause can be expected to form when the constituent material of a body is highly conducting or it possesses a conducting ionosphere, so that currents can flow through or around the body. Forces associated with these currents then impede the incoming flow.

Another relevant piece of physics that can be important is that of "draping" of magnetic field lines over a conducting obstacle, such as a magnetopause or

ionopause. This can lead to a substantial increase in magnetic field strength at the obstacle.

The physics of an ionopause and magnetic draping can be studied using the MHD equations of motion (2.24) and induction (2.34). We assume a simple 1D approximation to these equations to model this system, as illustrated in Figure 19.6. The steady solar wind plasma flows in the **z**-direction, with $\mathbf{U} = U(z)\,\hat{\mathbf{z}}$, and

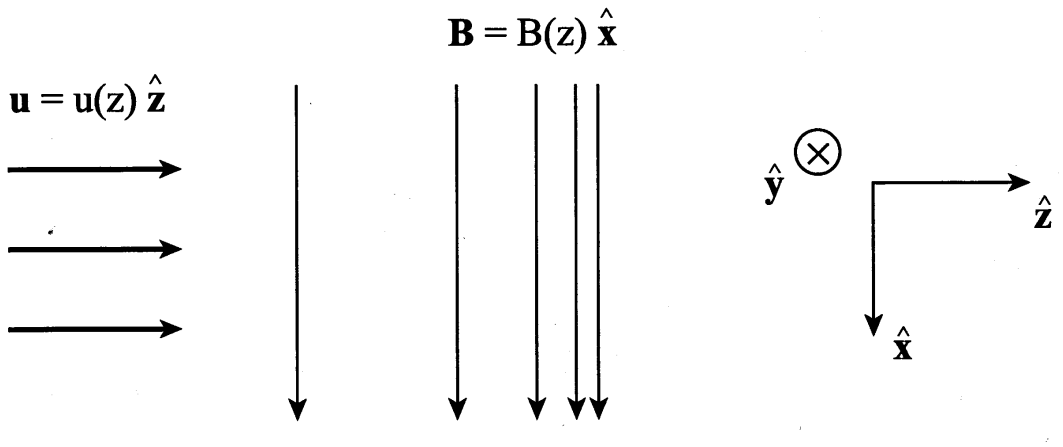


Figure 19.6: Geometry for 1D MHD model of the ionospause at Venus.

the interplanetary magnetic field lines point in the **x**-direction, where the magnitude of the field may vary in the **z**-direction, with $\mathbf{B} = B(z,t)\,\hat{\mathbf{x}}$. The induction equation then has the form

$$\frac{\partial B(z,t)}{\partial t} = -\frac{\partial}{\partial z}(UB) + \frac{1}{\mu_0 \sigma}\frac{\partial^2 B}{\partial z^2}\,, \tag{19.13}$$

where $\sigma$ is the conductivity coefficient. The first term on the right-hand side of the induction equation is the magnetic convection term and the second term is the magnetic diffusion term. For high-conductivity plasmas, the diffusion term is small and can be neglected. Recall from Lecture 2 that this approximation yields the condition for frozen-in magnetic flux. Equation (19.13), with $\sigma = \infty$, has the steady-state solution

$$U(z)B(z) = \text{constant}\,, \tag{19.14}$$

so that the frozen-in field lines bunch up in regions where the flow speed is small. This explains the magnetic enhancement in front of the ionopause in Figure 19.5, where the plasma flow has slowed down.

We seek a steady-state solution ($\partial/\partial t = 0$) of the MHD equation of motion (2.25), assuming charge neutrality ($\rho = 0$) and neglecting gravity, which gives

$$\eta U \frac{\partial U}{\partial z} = -\frac{\partial}{\partial z}\left(p_{th} + \frac{B^2}{2\mu_0}\right)\,. \tag{19.15}$$

It follows from the mass conservation equation (2.19) that

$$\eta U^2 + p_{th} + \frac{B^2}{2\mu_0} = \text{constant}\,. \tag{19.16}$$

This is an expression of the conservation of total pressure in the flow direction. The first term is the dynamic ram pressure of the solar wind, the second term is the thermal pressure, and the third term is the magnetic pressure. In the magnetic

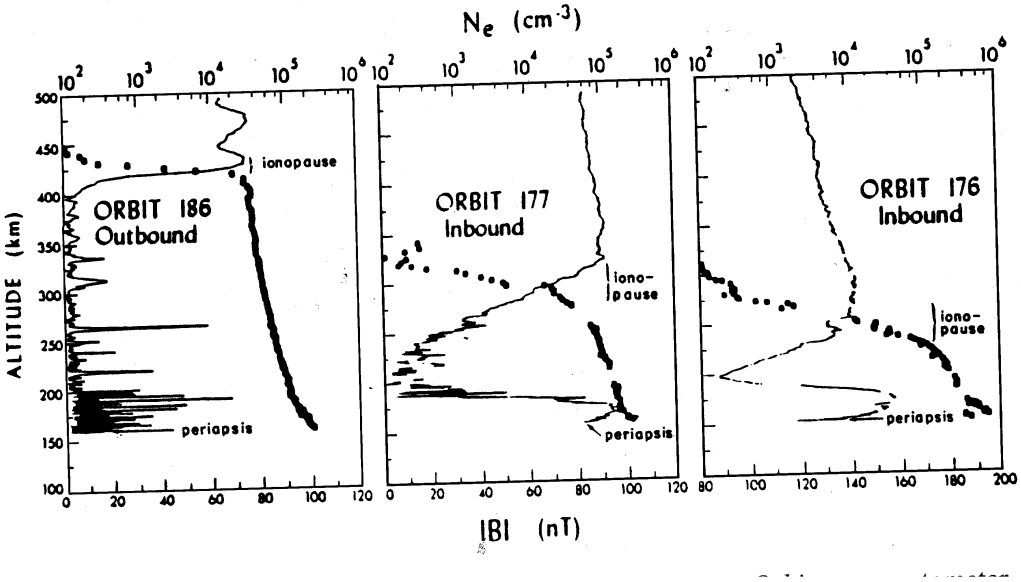


Figure 19.7: Pioneer Venus Orbiter (PVO) magnetometer data and measured electron number density (dots) in the ionosphere of Venus for three separate orbits (Russell and Vaisberg, 1983).

field build-up region in front of the ionopause, the magnetic pressure is high to compensate for the low ram pressure.

At the ionopause barrier (altitude $h = 425$ km), the flow velocity (in the $z$-direction) is zero, and the pressure balance equation (19.16) becomes

$$p_{th} + \frac{B^2}{2\mu_0} = \text{constant} \approx P_{ram,SW} \, . \tag{19.17}$$

The condition

$$p_{th,iono} \approx \frac{B^2}{2\mu_0} \approx P_{ram,SW} \tag{19.18}$$

must be satisfied at the interface between the low density, magnetized magnetosheath plasma and the dense, unmagnetized ionospheric plasma. Here $B$ is the magnetic field just on the solar wind side of the ionopause. Question 2 of Assignment 5 shows that the particle currents lead to the required $\mathbf{J} \times \mathbf{B}$ forces, consistent with the analyses in Lecture 13 for Earth's magnetopause.

Figure 19.7 shows magnetometer and plasma density data from the Pioneer Venus Orbiter for three orbits. The first panel corresponds to the most common situation where the ionosphere is unmagnetized.

Changes in the solar wind ram pressure cause the Venusian ionosphere to move up and down and to sometimes become magnetized, as implied by panels 2 and 3 in Figure 19.7. The physics is as follows. The stronger the ram pressure, the higher the magnetic field strength in front of the ionopause, due to conversion of ram pressure to magnetic pressure. From equation (19.18), the higher magnetic pressure in the static pressure balance at the ionopause must be balanced by the ionospheric thermal pressure $p = n_e k_B (T_e + T_i)$; i.e., a higher plasma density $n_e$ is needed to maintain the pressure balance. Recall from Lecture 16 that the ionospheric plasma is in local hydrostatic equilibrium; i.e., locally, the plasma density increases exponentially with decreasing altitude. Hence pressure balance is maintained by the ionopause moving down to a new pressure equilibrium position at lower altitudes.

This is evident in Figure 19.7, where the altitude of the ionopause decreases from 425 km for the unmagnetized ionosphere (first panel) to $\lesssim$300 km for the magnetized ionosphere (second and third panels).

Venus's ionosphere becomes magnetized (panels 2 and 3 in Figure 19.7) when the solar wind ram pressure is comparable to or greater than the ionospheric thermal pressure. The stronger the ram pressure, the higher the magnetic field strength in front of the ionopause, due to conversion of ram pressure to magnetic pressure. From equation (19.18), the higher magnetic pressure in the static pressure balance at the ionopause must be balanced by the ionospheric thermal pressure $p = n_e k_B(T_e + T_i)$; i.e., a higher plasma density $n_e$ is needed to maintain the pressure balance. Recall from Lecture 16 that the ionospheric plasma is in local hydrostatic equilibrium; i.e., locally, the plasma density increases exponentially with decreasing altitude. Hence pressure balance is maintained by the ionopause moving down to a new pressure equilibrium position at lower altitudes. This is evident in Figure 19.7, where the altitude of the ionopause decreases from 425 km for the unmagnetized ionosphere (first panel) to $\lesssim$300 km for the magnetized ionosphere (second and third panels).

Magnetization of the ionosphere is shown by the additional peak in magnetic field strength at low altitudes ($h = 175$ km). This can also be explained qualitatively with the 1D MHD model, in terms of magnetic flux being forced into Venus's ionosphere from the magnetic barrier in front of the ionopause when the solar wind ram pressure is large. The simplest physical picture is that non-zero magnetic fields are required in the ionosphere to maintain pressure balance in this case.

### Mars

Mars is essentially unmagnetized, like Venus, but with localized remnant magnetic fields associated with masscons or particular geological events. The ionopause is thus globally like that of Venus, but likely with time-varying perturbations associated with the remnant magnetic fields.

## Further reading:


1. Baganel, F., 1992, Giant planet magnetospheres, *Ann. Rev. Earth Planet. Sci.*, **20**, 289.
2. Brice, N. M. and Ioannidis, G. A., 1970, The magnetospheres of Jupiter and Earth, *Icarus*, **13**, 173.
3. Cravens, T. E., Shinagawa, H., and Nagy, A. F., 1984, The evolution of large-scale magnetic fields in the ionosphere of Venus, *Geophys. Res. Lett.*, **11**, 267.
4. Cravens, T. E., 1997, *Physics of Solar System Plasmas*, Cambridge University Press, Cambridge, Chapters 4, 7 and 8.
5. Kivelson, M. G. & Baganel, F. , 1999, Planetary magnetospheres, in *Encyclopedia of the Solar System*, (Eds. Weissman, P. R., McFadden, L-A, and Johnson, T. V.), Academic Press, San Diego, p. 477.
6. Russell C. T. and Vaisberg O., 1983, The interaction of the solar wind with Venus, in *Venus*, (Eds. Hunten, D. M., Colin, L., Donahue, T. M., and Moroz, V. I.), Univ. Arizona Press, Tucson, p. 183.
7. Russell, C. T., and Walker, R. J., 1995, The magnetospheres of the outer planets, in *Introduction to Space Physics*, (Eds. Kivelson, M. G. & Russell, C. T.), Cambridge University Press, Cambridge, Chapter 15.